Low-density electron-hole liquid in uniaxially compressed Ge

I. V. Kukushkin and V. D. Kulakovskiĭ

Institute of Solid State Physics, USSR Academy of Sciences
(Submitted 12 October 1981)
Zh. Eksp. Teor. Fiz. **82**, 900–914 (March 1982)

The decisive role played by band anisotropy in the stabilization of the metallic phase (of an electron-hole liquid (EHL)) in the case of nondegenerate parabolic bands is demonstrated, with an investigation of the condensation of excitons in Ge crystals strongly compressed along the axes ⟨111⟩ and ⟨~100⟩ as the example. The exciton binding energy in the EHL in Ge ⟨111⟩ is $\varphi \approx R/5$ (R is the exciton Rydberg). In pure Ge ⟨~100⟩, $\varphi \approx 1/2\Delta_M < R/10$ (Δ_M is the binding biexciton energy and to assess the stability of the EHL measurements at temperatures $T < 1$ K are necessary. It was observed that weak doping ($N \sim 3\times 10^{12}$ cm^{-3}) stabilizes the EHL in Ge⟨~100⟩; the density of the EHL is in this case $(7–8)\times 10^{15}$ cm^{-3} ($r_s \approx 1.8$). The role of the multiparticle effects in the formation of the EHL emission spectrum is found to increase with decreasing EHL density. A decrease in the stability of the EHL in Ge⟨~100⟩ with $N \sim 3\times 10^{12}$ cm^{-3} is observed in magnetic fields $H \approx 0.5$ T. This is explained within the framework of the total-density approximation for the exchange-correlation energy.

PACS numbers: 71.35. + z

§1. INTRODUCTION

A gas of nonequilibrium electrons in indirect semiconductors Si and Ge condenses at low temperatures into a dense metallic EHL with large binding energy $\varphi(\approx R/2)$ (see, e.g., the reviews[1,2]). Lifting the band degeneracy decreases φ (Ref. 3). It follows from calculations that in the case of nondegenerate isotropic electron and hole bands the metallic phase is less stable than the molecular phase.[1] Closest to this idealized model is uniaxially compressed Ge, which has simple but unfortunately anisotropic bands.[1)] It follows from theoretical calculations[5-7] that the anisotropy of the bands lowers the energy of the metallic state, and its value expected for Ge⟨111⟩ is close to $0.15R$. We recall that the binding energy Δ_M of the excitonic molecules (EM) in Ge amounts, according to calculations,[8] to $\Delta_M \approx 0.03R$, as a against $\Delta_M \approx 0.1R$ obtained in experiment.[9]

It is seen from the foregoing that investigations of the condensation in strongly compressed Ge crystals are most pressing from the point of view of destabilization of the metallic phase, the formation of which makes it impossible to investigate collective interactions in a dielectric exciton system of high density and, in particular, Bose-Einstein condensation. It is of considerable interest also to track the change of the role played by metallic-phase multiparticle effects in the formation of the emission spectrum with decreasing density of this phase. It is known that in a dense EHL, owing to the strong screening of the Coulomb potential, the role of such effects is extremely small (see, e.g., Ref. 1). The experimental difficulties encountered in this case lie mainly in obtaining very large homogeneous strains, so as to exclude the influence of the nonparabolicity of the valence band, which stabilizes strongly the EHL. To our knowledge, the maximum employed uniform pressure in Ge⟨111⟩ was $P \approx 140$ MPa, in which case the nonparabolicity of the valence band was still large and the binding energy φ of the EHL was larger than $0.3R$ (Ref. 10).

We have called attention in Ref. 11 to the possibility of obtaining a more promising exciton system in Ge⟨~100⟩,[2)] in which the anisotropy of the valence band is much lower than in Ge⟨111⟩. It was precisely in Ge⟨~100⟩ that it was possible to obtain in an exciton system, a chemical potential so large that the densities of the excitons and of the EM turned out to be comparable.

We investigate in this paper the condensation of excitons both in Ge⟨111⟩ (§§ 3, 5) and in Ge⟨~100⟩ (§§ 4–6) by analyzing the behavior of the allowed and forbidden components of the emission spectra of EHL, EM, and excitons when the excitation density, the temperature, and the strains are varied (§§ 3, 4, 6), when the impurity density is varied (§§ 4–6), and when a weak magnetic field is applied (§§ 5, 6).

§2. EXPERIMENT

To obtain a large sufficiently uniform uniaxial compression of the Ge crystals we used a procedure similar to that described earlier[12] for the compression of Si crystals. It must be emphasized that the requirements imposed on the uniformity of the strain of the Ge crystals in the study of a weakly bound EHL are extremely stringent. By virtue of the very small binding energy (~0.5 meV) and the large diffusion lengths of the electron-hole pairs (>1 mm) the inhomogeneity of the strain in the crystal must certainly not exceed 0.1–0.2%. Only in this case is a monotonic variation of the characteristics of the emission spectra observed with increasing strain. In the opposite case, the EHL and exciton emission lines begin to broaden already at $P \sim 150–200$ MPa. To obtain a highly uniform strain we placed in our setup, in contrast to that described in Ref. 12, not one but two liners of tin-lead alloy, 1.5 mm thick, between the plungers and the crystal. Prior to their placement, the mechanically polished crystals were etched in the polishing etchant CP-4a. A small initial strain was produced at room

 0038-5646/82/030528-09$04.00

temperature. The sample was indented thereby to a depth of ~1 mm in each of the liners. It was found empirically that at a crystal length 10 mm the best results are obtained for samples with cross sections 3×3 mm.

The procedure employed yielded uniform pressures $P \sim 400$ MPa in Ge⟨111⟩ and $P > 600$ MPa in Ge⟨~100⟩. (A higher uniformity is required in compression along the ⟨111⟩ axis because of the stronger dependence of the width of the forbidden band on the strain.) At $P \sim 500$ MPa the splitting of the valence band $\Delta E_v \approx 20$ meV, or $\approx 10 E_{Fh}$, where E_{Fh}(≈2 meV) is the energy of the Fermi holes in the EHL, and the nonparabolicity of the valence band at $E < E_{Fh}$ is small.

We investigated Ge with shallow-impurity density $N = 3 \times 10^{12}$ and 3×10^{11} cm^{-3}. The samples were placed in superfluid helium, thereby ensuring minimum overheating of the crystals. The heat rise, as follows from an analysis of the exciton emission line shape, decreases with increasing distance from the He λ point, and equals ~0.3 K at a bath temperature $T_b = 1.5$ K and at an average excitation power $W \sim 1$ W. The excitation was with a cw 1.06 μm laser with power up to 6 W, the emission of which was modulated by a mechanical chopper at an off-duty cycle from 1 to 1/6. To record the differential (with respect to the excitation density) spectra we used 20% modulation of the laser intensity.

The spectral instrument was a double monochromator with gratings of 600 lines/mm and dispersion 8 Å/mm. The radiation was registered with a cooled Ge(Cu) photoresistor and lock-in detector.

The magnetic field H was always parallel to the strain axis. The radiation was registered in Voigt's geometry ($\mathbf{H} \perp \mathbf{k}$).

§3. EHL IN Ge⟨111⟩

As noted in §2, we tracked the behavior of the emission spectrum in Ge⟨111⟩ up to $P \sim 350$ MPa. Under these conditions $\Delta E_v \simeq 14$ meV $\approx 7 E_{Fh}$ and the deviation of the state density at the Fermi level from its value in the limit of strong compression is approximately 15%. As the hole dispersion law approaches the square of the distance between the EHL emission lines (L) and of the exciton lines (FE) decreases and the relative intensity of the emission lines of the excitons increases (because of the decrease of the binding energy of the EHL), while the L line becomes narrower (because of the decrease of the EHL density) (Fig. 1). At larger strains, emission appears also in the region between the lines L and FE; it is natural to attribute this emission to radiative recombination of EM (EM → photon + phonon + exciton). Besides the spectral position, it has also a number of properties inherent in EM radiation, which was investigated in detail by us in Ge⟨~100⟩ (Refs. 9, 11), namely: it appears only at sufficiently large excitation densities near the condensation thresholds, and has the same width as the M emission line in Ge⟨~100⟩, its increase is faster than linear relative to the intensity of the emission of the excitons, and weakens strongly when a magnetic field $H \sim 1$ T is turned on (§ 5).

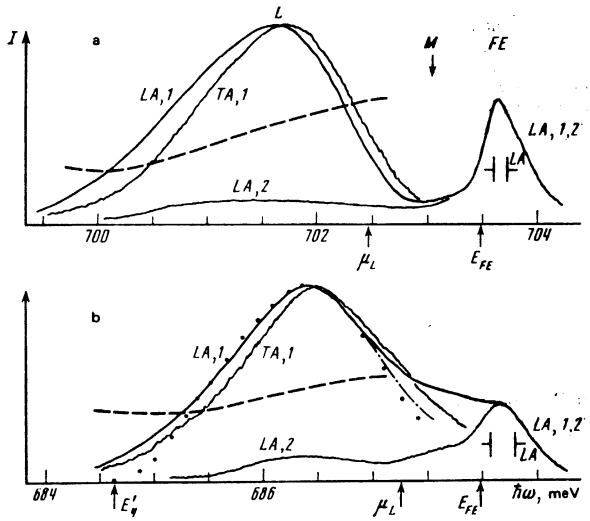

FIG. 1. Emission spectrum of Ge ⟨111⟩ in the forbidden (with TA phonon) and allowed (with LA phonon) components at $T_b = 1.7$ K, in the case of a weak (a, $P = 120$ MPa) and strong (b, $P = 320$ MPa) deformation, recorded at a high excitation density (1) and near the condensation threshold (2). For convenience in the comparison, the TA spectrum is shifted into the region of the LA component by an amount equal to the energy difference between the LA and TA phonons. The dashed curve shows the ratio I_{TA}/I_{LA}. The excitation densities are equal to: a) 1 (LA and TA) – $W = 20$ W/cm^2, 2 (LA) – $W = 4$ W/cm^2, b) 1(LA and TA) – $W = 150$ W/cm^2, 2 (LA – $W = 40$ W/cm^2. The dash-dot line in Fig. 1b shows the EHL emission line shape obtained from the difference of the spectra 1 and 2 of LA, normalized to the emission line of the excitons, while the points were calculated using expression (2).

Figure 1 shows also the forbidden components of the EHL emission line in Ge⟨111⟩ (with emission of a TA phonon). For convenience in the comparison of the allowed and forbidden components, the TA spectrum is shifted relative to the LA spectrum by an amount equal to the phonon energy difference $\hbar\Omega^{LA} - \hbar\Omega^{TA} = 19.78$ meV. For the TA spectrum, the matrix element of the transition differs from zero if the electron or hole is located not at symmetrical points (Δ and Γ respectively)[1]:

$$\mathbf{M}_{TA}(\mathbf{k}_e, \mathbf{k}_h) = \mathbf{M}_{TA}{}^{e}\mathbf{k}_e + \mathbf{M}_{TA}{}^{h}\mathbf{k}_h. \qquad (1)$$

It is seen from Fig. 1 that for the EHL the ratio I_{TA}/I_{LA} increases with increasing $\hbar\omega$ because of the increase of the quasimomenta of the recombining electrons and holes.

To determine the EHL parameters from the shape of the emission spectrum, we used an expression obtained in the single-particle approximation[1]:

$$I(h\nu) = \int_0^{h\nu} |\mathbf{M}|^2 D_e(E) D_h(h\nu - E) f_e(E, E_{Fe}, T) f_h(E - h\nu, E_{Fh}, T)\, dE, \qquad (2)$$

Here $h\nu$ is reckoned from $E'_g - \hbar\Omega_{TA(LA)}$, E'_g is the renormalized width of the forbidden band, and $f_{e(h)}$ and $D_{e(h)}$ are respectively the distribution functions and state densities of the electrons (holes). This expression describes well the emission line shape of a dense EHL with $r_s = (3/4\pi n_0 a_{ex}^3)^{1/3} \lesssim 1$ (see, e.g., Ref. 2).

From an analysis of the influence of the multiparticle corrections on the shape of the emission spectrum[1,13,14] it follows that it is small because of the short-range character of the screened Coulomb interaction. We introduce the parameter

$$\zeta = \frac{I_{TA}(0)/I_{LA}(0)}{I_{TA}(E_{Fe}+E_{Fh})/I_{LA}(E_{Fe}+E_{Fh})}$$

Within the framework of the single-particle approximation, this parameter vanishes by virtue of the equation $\mathbf{M}_{TA}(\mathbf{k}_e = 0, \mathbf{k}_h = 0) = 0$. In the case of a dense EHL with $r_s \lesssim 1$, the contribution from the multiparticle corrections produces a small low-energy tail of the line L, due primarily to the plasma excited states and to a lesser degree to the excitation of extra electrons or holes and to the damping of the single-particle states far from the Fermi level.[1] These processes are accompanied by transfer of part of the energy and of a certain quasimomentum to a third particle. They influence particularly strongly the form of the red edge of the forbidden component, where in the single-particle approximation the matrix element tends to zero. As a result, the parameter ζ introduced above differs from zero.

From a comparison of the TA and LA emission spectra of the EHL in undeformed germanium it follows that $\zeta \approx 0.05$. The value of ζ increases in uniaxially compressed Ge⟨111⟩ crystals. It is seen from Fig. 1 that $\zeta \approx 0.4$ at $P \approx 120$ MPa and $\zeta = 0.65$ at $P \approx 320$ MPa. So great an increase of the influence of the multiparticle corrections on the EHL line shape in compressed crystals is due to the decrease of the EHL density. In light of the analysis[1,13,14] of the limits of applicability of the single-particle approximation, this result is natural, since the Coulomb-interaction screening length increases with decreasing density of the electron-hole (e-h) pairs.

It follows from the foregoing that in strongly compressed Ge crystals, when the expression (2) is used to approximate the EHL emission line shape, the error in the determination of the EHL parameters (the chemical potential μ_L, the electron and hole Fermi energies E_{Fe} and E_{Fh}, and the density n_0) turns out to be noticeably larger than in undeformed Ge. We note that expression (2) is more suitable for the description of the allowed component, for which M is constant, and the influence of the numerous corrections on the red edge is much smaller than for the forbidden component. The error in μ_L, which is determined from the violet boundary of the spectrum, remains small.

From the analysis of the allowed components of the L line in Ge⟨111⟩ at $T_b = 1.7$ K ($T_{ex} = 2$ K) and $P \approx 120$ MPa (Fig. 1) we found that the chemical potential μ_L, reckoned from the exciton term, is $\mu_L = -1.0 \pm 0.1$ meV. When P increases to 320 MPa, μ_L decreases to 0.7 ± 0.1 meV, or $\approx R/4$, and the density decreases to $(1.1 \pm 0.1) \times 10^{16}$ cm^{-3} ($r_s \approx 1.6$). In the approximation of the experimental curve (Fig. 1) we have assumed that the EHL temperature is equal to the exciton temperature T_{ex} obtained from an analysis of the exciton emission line with account taken of the spectral width of the gap at medium strains ($P = 120$–140 MPa), when the FE line is well resolved at all excitation densities and has a Boltzmann contour with half-width $1.8kT_{ex}$. Since it is possible to describe adequately the red edge of the L line, we started from the condition that the half-widths of the experimental and calculated emission spectra of the EHL are equal. The obtained values of μ_L and n_0 are close to those calculated by Vashishta *et al.*[6,7] (Table I) using the self-consistent scheme of Singwi *et al.*[15]

TABLE I. EHL parameters in strongly compressed Ge⟨~100⟩ and ⟨111⟩.

	Ge ⟨111⟩			Ge ⟨~100⟩				
	Theory[7]		Experiment	Theory			Experiment	
$\Delta E_g/E_{Fh}$	∞	∞	7	∞ *	∞ **	∞ **	12	
T, K	0	2	2	0	0	1.75	1.75	2.8
$-\mu_L$, meV	0.426	0.54	0.7	0.21	0.19	0.27	0.28	0.37
$-\mu_{ex}$, meV	–	–	0.7	–	–	–	0.34	0.43
$-\mu_L+R$, meV	3.08	3.2	3.35	3.01	2.99	3.07	3.08	3.17
$n_0 \cdot 10^{-15}$, cm^{-3}	11.1	8.9	11	10.1	9.7	8.2	7.3	6.5
r_s	1.58	1.69	1.58	1.63	1.65	1.73	1.81	1.88
$E_{Fe}+E_{Fh}$, meV	2.88	2.46	2.7	2.84	2.76	2.44	2.16	2.02
$n_g \cdot 10^{-15}$, cm^{-3}	–	0.4	0.12	–	–	1.7	0.94	2.8

*A calculation using the $\mathscr{E}_{xc}^{0}$ dependence from Ref. 6.
**Calculation using $\mathscr{E}_{xc}^{\langle 111\rangle}$ from Ref. 6.

Since excitons and EM are present in the gas phase of Ge⟨111⟩, the ratio of their integrated emission intensities I_M/I_{FE} in the spectrum near the condensation threshold can be used to estimate independently the chemical potential in the gas phase

$$\mu_g = \mu_{ex} = 1/2\mu_M. \tag{3}$$

From (3), recognizing that the degeneracy multiplicity of the exciton term is four times larger, and the exciton state-density mass is two times larger than for EM, it follows that

$$\frac{I_M}{I_{FE}} = \alpha \frac{n_M}{n_{FE}} = 2^{3/2}\alpha \exp\left(-\frac{|\mu_{ex}|-\Delta_M}{kT}\right). \tag{4}$$

The EM binding energy is here $\Delta_M = 0.27 \pm 0.06$ meV,[9] and the ratio of the radiative probabilities for the EM and for the excitons[3] is $\alpha \approx 2$. From Fig. 1(b) (curve LA, 2) it is seen that $I_M/I_{FE} \approx 1/3$–$1/4$, from which it follows that $\mu_{ex} = -0.7 \pm 0.15$ meV. The error in μ_{ex} is small, since the ratio I_M/I_{FE} enters logarithmically. The agreement between μ_L and μ_{ex} is evidence of thermal equilibrium between the gas and the EHL.

§4. EHL IN Ge ⟨~100⟩ WITH IMPURITY DENSITY 3×10^{12} cm^{-3}

In Ge⟨~100⟩, which differs from Ge⟨111⟩ only in the smaller anisotropy of the valence band, the gas-phase density, as found in Ref. 9, is substantially higher. In the present paper we trace the EHL radiation. Figure 2 shows the variation of the emission spectra of Ge⟨~100⟩ with $N = 3 \times 10^{12}$ cm^{-3} as the pressure is increased to $P = 480$ MPa. The TA and LA spectra were recorded at a bath temperature $T_b = 1.6$ K and an excitation density $W = 30$ W/cm^2. With increasing strain, the intensity of the L line decreases and it vanishes completely at the maximum strains. With increasing excitation density, however, it again appears in the spectrum [Fig. 2(c), spectra TA° and LA°, recorded at[4)] $W = 200$ W/cm^2].

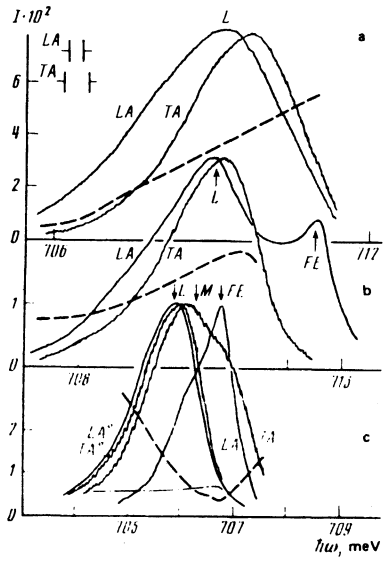

FIG. 2. Emission spectra of Ge ⟨~100⟩ with $N = 3 \times 10^{12}$ cm^{-3} in the forbidden (TA) and allowed (LA) components at $T_b = 1.6$ K and different strains: a) $P = 50$ MPa, b) $P = 160$ MPa, and c) $P = 480$ MPa. The TA and LA spectra were recorded at $W = 30$ W/cm², $TA°$ and $LA°$, at 200 W/cm², For convenience in comparison the TA spectra are shifted into the region of the LA component by an amount equal to the difference between the energies of the LA and TA phonons. The dashed curves show the ratio I_{TA}/I_{LA}, and the dash-dot curves the ratio $-I_{TA}°/I_{LA}°$. The scale on the ordinate axis pertains to the ratio I_{TA}/I_{LA}.

The ratio I_{TA}/I_{LA} for excitons increases with increasing $\hbar\omega$ [Fig. 2(c)] in accordance with the increase of the ratio of the matrix elements $|\mathbf{M}_{TA}|^2/|\mathbf{M}_{LA}|^2 \sim \mathbf{K}_{ex}^2 \sim \hbar\omega - E_{ex}$. For biexcitons this ratio, on the contrary, increases with decreasing $\hbar\omega$ by virtue of the increase of the quasimomentum of the recoil exciton [Fig. 2(c), see also Ref. 9]. The dependence of I_{TA}/I_{LA} for EHL in strongly compressed Ge⟨~100⟩ crystals, just as in Ge⟨111⟩, becomes extremely weak [Fig. 2(c)], thus indicating a strong influence of the multiparticle correlations on the line shape. It is also seen from Fig. 2 that owing to the decrease of the Fermi momentum in the EHL the ratio I_{TA}/I_{LA} decreases strongly on the violet edge of the L line. At $P \approx 500$ MPa it turns out to be noticeably smaller than on the red edge of the M line, when the exciton-recoil kinetic energies close to E_{Fh}. This difference is apparently due to the opening up, upon recombination of the EM, of a larger quasimomentum region, despite the participation of particles having the same energy as in the recombination of electrons and holes into EHL, owing to the inequality of the translational masses of the exciton and the holes ($m_{ex} > m_h$).

It is seen from Fig. 2 that in strongly compressed Ge⟨~100⟩ the L and M lines overlap strongly. To separate the L line, whose appearance in the spectrum has a threshold, we used 20% modulation of the exciting light (Fig. 3). From a comparison of the spectra recorded with 100% (curve 1) and 20% (1′) modulation at low excitation density ($W \approx 30$ W/cm²), it is seen that a threshold exists for the appearance of the L line in the spectrum. At large W the difference between the usual (2) and differential (2′) spectra is small because the radiation intensities of the EM and of the excitons are low.

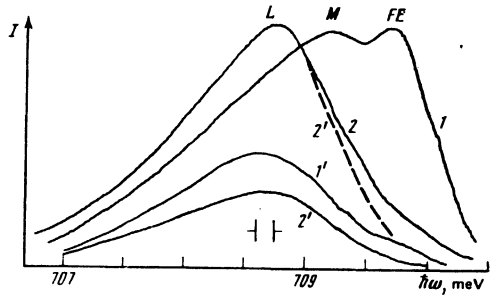

FIG. 3. LA spectra of the emission of weakly doped Ge ⟨~100⟩ at $P = 330$ MPa and $T_b = 1.6$ K near the condensation threshold (1, $W = 30$ W/cm²) and high excitation density (2, $W \sim 150$ W/cm²), recorded with 100% modulation (curves 1 and 2) and 20% modulation (curves 1′ and 2′) of the exciting light. The gain was not changed when the differential spectra were recorded. The spectrum 2′, shown dashed, is normalized to the maximum of curve 2.

To find the chemical potential and the EHL density in Ge⟨~100⟩ we approximated, just as in the case of Ge⟨111⟩, the form of the allowed (LA) component of the L line with the aid of expression (2) [Fig. 4(a)]. At $T_{ex} = 1.75$ K, the agreement between the calculated and experimental spectra is satisfactory at $\mu_L = -0.28 \pm 0.04$ meV $\approx 0.1R$ and $n_0 = (7.3 \pm 0.5) \times 10^{15}$ cm^{-3} ($r_s = 1.81$). For the chemical potential of the excitons in the gas phase we obtained, from the experimental value of I_M/I_{FE} at the condensation threshold [$I_M/I_{FE} \approx 2$, Fig. 4(a)], using Eq. (3), the close value $\mu_{ex} = -0.34 \pm 0.08$ meV.

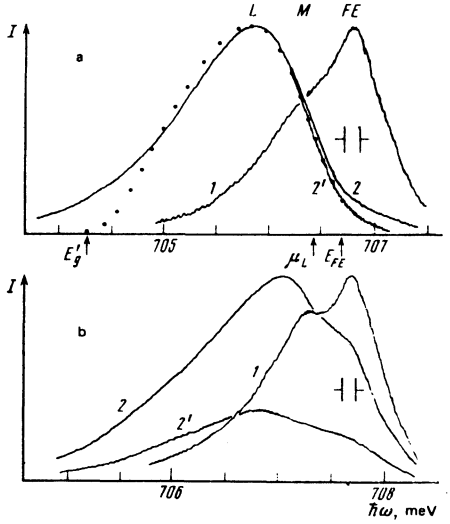

FIG. 4. LA spectra of the emission of strongly compressed Ge ⟨~100⟩ crystals with $N = 3 \times 10^{12}$ cm^{-3} (a) and 3×10^{11} cm^{-3} (b) at $T_b = 1.5$ K near the condensation threshold (curve 1) and at high excitation density (curves 2). The spectra (2′), which are differential in the density, were recorded at 20% modulation, and the amplification coefficient was ×2.5 for Fig. 4a and ×1 for Fig. 4b. The points on Fig. 4a shows the approximation of the shape of the EHL spectrum with the aid of expression (2) at $T_{ex} = 1.75$ K, $n_0 = 7.3 \cdot 10^{15}$ cm^{-3}. The pressures and excitation densities for the spectra are respectively: a) $P = 450$ MPa, $W = 40$ W/cm² (1) and 150 W/cm², (2), b) $P = 420$ MPa, $W = 70$ W/cm² (1) and 200 W/cm² (2).

The experimental parameters of the EHL in Ge⟨~100⟩ and Ge⟨111⟩ are compared in Table I with those calculated for $T = 0$ and $T = 2$ K, since the temperature corrections are substantial. The theoretical parameters for the EHL in Ge⟨~100⟩ were calculated by us using for the exchange-correlation energy $\mathscr{E}_{xc}(r_s)$ the relations calculated in Refs. 6 and 7 within the framework of the scheme of Singwi *et al.*[15] for Ge⟨111⟩ ($\mathscr{E}_{xc}^{(111)}$) and for the idealized band structure (simple isotropic parabolic bands) ($\mathscr{E}_{xc}^{0}$). As expected from the very weak sensitivity of $\mathscr{E}_{xc}(r_s)$ to the details of the band structure, the EHL parameters calculated using $\mathscr{E}_{xc}^{0}$ and $\mathscr{E}_{xc}^{(111)}$ differ very little. It is seen from the table that the experimental value of the chemical potential in Ge⟨~100⟩ agree well with the calculated ones, whereas the density of the EHL is noticeably lower than the theoretical value. It is not excluded, however, that neglect of the multiparticle effects (e.g., of the contribution from the vertex corrections that increase the recombination probability for electrons and holes as their energy approaches E_F, Refs. 14 and 17) the experimental value of n_0 is somewhat underestimated. From a comparison of the change of μ_L on going from Ge⟨111⟩ to Ge⟨~100⟩ it is seen that it is ≈0.15 meV smaller for the calculated values than the for the experimental ones. To a considerable degree, however, this discrepancy is due to the smaller strain in the Ge⟨111⟩ crystals, where $P \simeq 320$ MPa. At equal values of P (320 MPa) this discrepancy is decreased by almost 0.1 meV and lies within the limits of the experimental error. We note in this connection that in the case of Ge⟨111⟩ one should expect approximately the same decrease (i.e., ≈0.1 meV) of $|\mu_L|$ as obtained by us at P = 320 MPa, owing to the decreased nonparabolicity of the valence band with further increase of the degree of uniaxial deformation. The value $\mu_L = -0.6$ meV obtained for Ge⟨111⟩ by this extrapolation agrees well with the calculation. We call attention to the fact that the EHL binding energy (in Rydbergs) in Ge⟨111⟩ turns out to be somewhat larger than in Si⟨100⟩ ($\varphi = 0.17R$, Ref. 16), where the conduction band contains two valleys rather than one, but with small anisotropy. From the results above it follows that calculations of the EHL parameters with the correlation energy obtained by the method of Singwi *et al.*[15] describe well the experimental results both in Ge⟨111⟩ and in Ge⟨~100⟩.

§5. INFLUENCE OF WEAK MAGNETIC FIELDS ON EHL IN UNIAXIALLY COMPRESSED Ge

In strong magnetic fields, the dominant effect, as follows from the calculations[18] and the experiments in undeformed Ge,[19,20] is the decrease of the contribution made to the total EHL energy E_G by the kinetic energy of electrons and holes, owing to the increase of the state density at the bottom of the band because of the quantization of their motion. As a result, n_0 and $E_G(H)$ reckoned from $E_g(H)$ increase strongly in a magnetic field. The increase in the binding energy is in this case somewhat slower because of the increase of the exciton binding energy. In weak fields, however, one can expect a decrease of the stability of the EHL because of the lifting of the spin degeneracy in the bands,

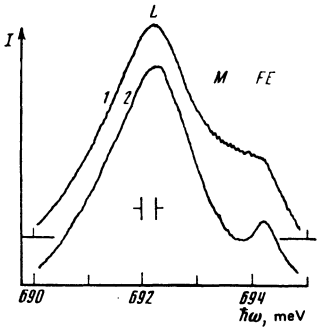

FIG. 5. Influence of magnetic field on the *LA* spectrum of the emission of strongly compressed pure crystals Ge⟨111⟩: 1—$H = 0$, 2—$H = 0.4$ T; $T_b = 1.7$ K.

if it is recognized that the Zeeman splittings for the electrons (holes) in the EHL and excitons are close. We turn now to the experimental results.

a. Ge⟨111⟩. In the study of the influence of the magnetic field on the emission spectra of Ge⟨111⟩ we have observed no oscillations in the intensity of either the exciton line or of the EHL emission line. With increasing magnetic field, a weak decrease of the relative intensity of the *FE* line is observed, as well as a strong decrease of the intensity of the EM radiation, which is located between the *L* and *FE* lines (Fig. 5). The change of the EHL binding energy is of the order of the error in its determination (~0.1 meV). The small decrease of I_{FE} is easily explained as being due to lifting of the degeneracy of the exciton term. At $H = 1$ T its splitting is comparable with kT: the split levels are located at 0.7, 3.3, and 4 K. Just as in Ge⟨~100⟩ (Ref. 9), the influence of the magnetic field on the EM density is substantially stronger, because of the impossibility of binding into an EM two excitons with electrons (holes) in identical spin states.

b. Ge⟨~100⟩. The behavior of the emission spectra of weakly compressed Ge⟨~100⟩ crystals with $N = 3 \times 10^{12}$ cm^{-3}, when the EHL binding energy is 0.7–1.2 meV, is perfectly analogous to that observed in strongly compressed Ge⟨111⟩ crystals. In more strongly com-

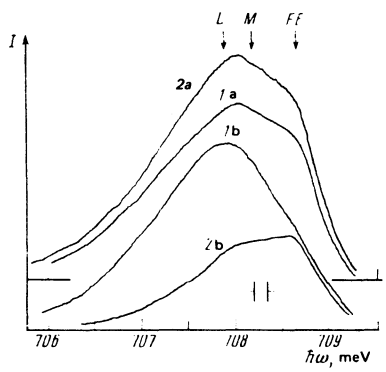

FIG. 6. Comparison of the emission spectra in a zero magnetic field (curve 1) and in a field $H = 0.4$ T (curves 2) of pure ($N = 3 \cdot 10^{12}$ cm^{-3}) (curves a) and weakly doped ($N = 3 \cdot 10^{11}$ cm^{-3}) (curves b) strongly compressed ($P = 380$ MPa) Ge⟨~100⟩ crystals at $T_b = 1.75$ K. The excitation density is 200 W/cm^2 for pure and 60 W/cm^2 for weakly doped crystals.

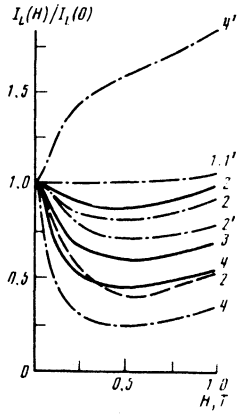

FIG. 7. Change of the radiation intensity in the region of the L line (at $\hbar\omega = E_{ex} - 1.5$ meV) upon variation of the temperature and pressure in pure (primed numbers) and weakly doped Ge⟨~100⟩ crystals. Solid line—T_b 1.5 K, dashed line—T_b = 1.75 K, and dash-dot line—T_b 2.50 K. The numbers correspond to different pressures: 1—P 220, 2—P 280, 3—P = 380 and 4—P 480 MPa.

pressed Ge⟨~100⟩ crystals, however, the influence of fields $H \sim 0.5$ T on the emission spectrum is quite substantial (Fig. 6): the EHL emission intensity decreases strongly, and the intensities of the EM and exciton emissions increase. Figure 7 illustrates the change of the intensity of the radiation in the region of the L line (at $\hbar\omega = E_{ex} - 1.5$ meV) upon variation of the temperature and pressure. The influence of the magnetic field on I_L is stronger the higher the pressure and temperature. Thus, at $P = 480$ MPa and $T_b = 2.1$ K the value of I_L decreases by a factor of 1.5 in a field $H = 0.05$ T. This result is qualitatively quite natural: the influence of the magnetic field increases with decreasing binding energy of the EHL and as the critical temperature is approached.

It is seen from Fig. 7 that in fields $H < 1$ T no oscillations are observed in the $I_L(H)$ dependence in Ge⟨~100⟩, despite the repeated crossing of the Landau levels by the Fermi quasilevels in this field interval. It follows therefore the observed change of the EHL stability is not connected with the effects of the de Haas–van Alphen type, which were observed earlier and investigated in detail in undeformed Ge in fields $H > 1$ T (Refs. 19, 21).

To describe the change of the EHL stability, we turn to consideration of the influence of the magnetic field on the ground states of the exciton, the EM, and the EHL. It is known that in weak fields we can write for the exciton and for the EM

$$E_{ex}(H) = E_{ex}(0) \pm {}^1/_2 (g_e \pm g_h)\mu_B H + {}^1/_2 \chi_{ex} H^2, \quad (5)$$

$${}^1/_2 E_M(H) = E_{ex}(0) - {}^1/_2 \Delta_M + {}^1/_2 \chi_M H^2, \quad (6)$$

where χ_{ex} and χ_M are the diamagnetic susceptibilities of the excitons and of the EM, which amount in Ge⟨~100⟩ to $\chi_{ex} = 0.35$ and $\chi_M = 0.94$ meV/T^2, respectively.[9,22]

The main difficulty in the calculation of the dependence of the ground state $E_G(n_0, H)$ of the EHL lies in the calculation of the correlation energy. It follows from experimental investigations of the behavior of Ge crystals, however, that the changes of the exchange and correlation energies in a magnetic field cancel each other to a considerable degree, so that when describing the experimental results up to fields $H = 18$ T one can neglect the dependence of the exchange-correlation energy on the magnetic field.[20] It is therefore natural to assume that in the weak-field case of interest to us, $H \leq 1$ T, the dependence of $\mathscr{E}_{xc}$ on H in Ge⟨~100⟩ can also be neglected compared with the change of $\mathscr{E}_{kin}(H)$. In this approximation, the contribution of $\mathscr{E}_{xc}$ to the diamagnetic susceptibility of the EHL is due only to the change of the total EHL density in the magnetic field. At very low temperatures the pressure p_g in the gas phase is small, and the change of the EHL parameters in the magnetic field can be obtained by assuming that the pressure in the EHL is $p_L = 0$ (Ref. 1). For convenience in the calculations, we can represent p_L and μ_L as sums of contributions from the gas of noninteracting particles $p_{e,h}(E_{Fe,h})$ and from the exchange-correlation energy $p_{xc}(\mu_{xc})$:

$$p_L = p_e + p_h + p_{xc}, \quad (7)$$

$$\mu_L = E_{Fe} + E_{Fh} + \mu_{xc}, \quad (8)$$

where

$$\mu_{xc} = \mathscr{E}_{xc} + n\partial\mathscr{E}_{xc}/\partial n, \quad p_{xc} = n^2\partial\mathscr{E}_{xc}/\partial n. \quad (9)$$

In strongly compressed ($P \sim 500$ MPa) Ge⟨~100⟩ crystals in fields $H \lesssim 1$ T, the nonparabolicity of the valence band can be neglected, since the corrections $\Delta\hbar\omega_c/\hbar\omega_c$ near E_{Fh} do not exceed 10%, (see, e.g., Ref. 23). Here $\hbar\omega_c$ is the cyclotron frequency. In this case $p_{e,h}(H)$ is given by

$$p_{e,h} = \frac{eHm_z^{1/2}(2kT)^{1/2}}{(2\pi\hbar)^2} \times \sum_{n=0}^{\infty}\sum_{s_z=\pm 1/2}\int_0^{\infty} \frac{z^{1/2}dz}{1+\exp\{z-[\mu-\hbar\omega_c^{e,h}(n+{}^1/_2)+s_z\mu_B g_{e,h}H]/kT\}}, \quad (10)$$

where $g_{e,h}$ are the g factors and $m_z^{e(h)}$ is the effective mass of the electron (hole) in the EHL along the magnetic field.

Expansion of expression (10) in powers of the small parameter $\hbar\omega_c^{e,h}/E_{Fe,h}$ at $T = 0$ yields

$$p_{e,h}(H) = p_{e,h}(0)\left\{1 - \frac{5}{32}\left(\frac{\hbar\omega_c^{e,h}}{E_{Fe,h}}\right)^2 + \frac{15}{32}\left(\frac{g_{e,h}\mu_B H}{E_{Fe,h}}\right)^2\right\}, \quad (11)$$

where

$$p_{e,h}(0) = \frac{2^{3/2}(m_{de,h})^{3/2}}{15\pi^2\hbar^3}E_{Fe,h}^{5/2}$$

is the pressure at $H = 0$ and $T = 0$. It is seen from (11) that there are no corrections linear in the magnetic field to $p_{e,h}$. The quadratic corrections for a free-electron gas are well known. They are connected with the Landau diamagnetism and the Pauli paramagnetism, and by virtue of the equality $\hbar\omega_c = g_e\mu_B H$ the diamagnetic correction prevails for free electrons.[24] The situation is different in the case of EHL in Ge⟨~100⟩, where the diamagnetic correction predominates by virtue of the smallness of the g-factors $g_{e,h}$ compared with the reciprocal cyclotron masses ($m_{ce,h}^{-1}$).

From the condition $p_L = 0$ at $T = 0$ we get

$$\frac{\partial p}{\partial n}\Big|_{n=n_0} \Delta n \approx \frac{5}{32}\sum_{i=e,h} p_i(0)\left(\frac{\hbar\omega_c^i}{E_{Fi}}\right)^2, \qquad (12)$$

whence for a ground state energy $E_G(H) \equiv \mu_L(H)|_{T=0}$, taking into account the relations

$$\partial p/\partial \mu = n \qquad (13)$$

and

$$p_i(0) = {}^2/_5 n E_{Fi}, \qquad (14)$$

we obtain

$$\mu_L(H) = E_G(H) = E_G(0) + {}^1/_2 \chi_L H^2, \qquad (15)$$

where the diamagnetic susceptibility per e-h pair is

$$\chi_L \approx \frac{1}{8}\sum_{i=e,h}\frac{(\hbar\omega_c^i)^2}{H^2 E_{Fi}} = \frac{1}{4}\frac{e^2}{c^2(3\pi^2 n_0)^{1/3}}\left[\frac{m_{de}}{m_{ce}^2} + \frac{m_{dh}}{m_{ch}^2}\right]. \qquad (16)$$

We did not write out the paramagnetic term, which is small in Ge⟨~100⟩. It is seen from (16) that χ_L increases with decreasing EHL density. From the calculation of χ_L for the EHL in Ge⟨~100⟩ at $T = 0$ it follows that $\chi_L = 0.29$ meV/T^2, and the main contribution to χ_L is made by the electrons. It is seen that χ_L is close to the diamagnetic susceptibility of the excitons and of the EM.

From a comparison of the magnetic-field dependences of U_{ex}, E_M, and E_G [Eqs. (5), (6), and (15)] it follows that in the weak-field limit the binding energy of the excitons in the EHL will decrease because of the presence of the linear term in the $E_{ex}(H)$ dependence (Fig. 8). However, by virtue of the inequality $\chi_L < \chi_{ex}$, the binding energy of the excitons in EHL will increase in strong magnetic fields.

At very low temperatures one can neglect the pressure of the exciton gas. In this case, by virtue of the appearance of a temperature increment $n\pi^2T^2/4E_{Fi}$ (at $kT \ll E_{Fi}$) in expression (14) for the pressure, it is necessary to replace E_{Fi} by $E_{Fi}(1 - \pi^2T^2/2E_{Fi}^2)$ in the quantity χ_L in expression (15) for the chemical potential μ_L. Consequently, the effect of the magnetic field on the chemical potential of the EHL increases with rising temperature, in qualitative agreement with experiment.

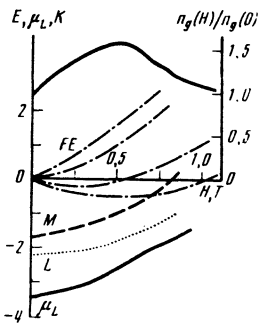

FIG. 8. Change of the energies of the ground state of the excitons (FE), EM (M), and EHL at $T = 0$ K (L) and of the chemical potential of the EHL at $T = 2$ K (μ_L) for Ge⟨~100⟩ in a magnetic field. The solid line in the upper part of the figure shows the calculated dependence for an equilibrium density of the gas phase at 2 K.

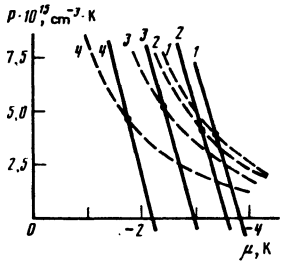

FIG. 9. Dependences of the pressure on the chemical potential for the EHL (solid lines) and for the gas phase (dashed) in Ge⟨~100⟩ at $T = 2$ K and in different magnetic fields: 1) $H = 0$, 2) $H = 0.2$ T, 3) $H = 0.5$ T, 4) $H = 0.8$ T. The curve intersection points correspond to equilibrium values of μ_L and p_L.

For quantitative calculations, at the fields $H \lesssim 1$ T and temperatures $T = 2$–3 K of interest to us, the approximate formulas obtained above turn out, however, to be too rough. Thus, the expansion parameters are $\hbar\omega_c/E_{Fi} \sim 1$ at $H \sim 1$ T and $kT/E_{Fe} \approx 0.3$ at 2 K. In addition, as shown by estimates, the gas-phase pressure is no longer negligibly small. To calculate $\mu_L(H)|_T$ we therefore used a numerical solution of the equation

$$p_g(\mu, H)|_T = p_{ex}(\mu, H)|_T + p_M(\mu, H)|_T = p_L(\mu, H)|_T. \qquad (17)$$

From the obtained chemical potential of the system ($\mu_g = \mu_L$) we calculated next the change in the gas-phase density $n_g = n_{ex} + 2n_M$. For an ideal gas of excitons and EM[5]

$$p_g = \frac{2}{5}(kT)^{5/2}\frac{m_{ex}^{3/2}}{\pi^2\hbar^3}\left\{\left[\sum_{i=1}^{4} B_{3/2}\left(\frac{x_i}{kT}\right)\right] + 2^{3/2}B_{3/2}\left(\frac{x_M}{kT}\right)\right\}, \qquad (18)$$

$$n_g = \frac{1}{\sqrt{2}}\frac{(m_{ex}kT)^{3/2}}{\pi^2\hbar^3}\left\{\left[\sum_{i=1}^{4} B_{1/2}\left(\frac{x_i}{kT}\right)\right] + 2^{1/2}B_{1/2}\left(\frac{x_M}{kT}\right)\right\}. \qquad (19)$$

The first term describes the contribution for the excitons ($x_i = \mu_L \pm \frac{1}{2}\mu_B(g_e \pm g_h)H + \frac{1}{2}\chi_{ex}H^2$), the second from the EM ($x_M = 2\mu_L - \Delta_M + \frac{1}{2}\chi_M H^2$), and m_{ex} is the exciton state-density mass, and

$$B_j(x_i) = \int_0^\infty \frac{z^j dz}{\exp(z - x_i) - 1}.$$

The calculation results are shown in Fig. 9. In the calculation of the contribution made to p_L by the exchange-correlation energy we used the $\mathscr{E}_{xc}(r_s)$ dependence for Ge⟨111⟩ from Ref. 6. We note, however, that the choice of $\mathscr{E}_{xc}(r_s)$ is not critical, for by virtue of the small change of μ_L in a magnetic field $H < 1$ T it suffices to know the first derivative $\partial p/\partial\mu$, which according to (14) is equal to the equilibrium density $n_0|_{H=0}$. It is seen from Fig. 8 that a maximum decrease of the EHL stability and an increase of n_g are expected at $H = 0.4$–0.6 T. In strong fields, the stability of the metallic phase should increase, in good agreement with experiment. We note also that allowance for the change of the pressure of the gas phase has led to an additional increase of $\mu_L(H)$, as a result of which in weak fields, $H \lesssim 0.2$ T, χ_L was compared with $\chi_M/2$. Accordingly, the ratio I_M/I_{FE} observed in experiment at $H = 0.4$ T (Fig. 4) is even somewhat larger than at $H = 0$. The accuracy of n_g, however, is insufficient for a correct quantitative comparison with calculation.

§6. FEATURES OF CONDENSATION IN PURE Ge ⟨~100⟩

In the preceding section we discussed the condensation of excitons in Ge⟨~100⟩ with impurity density $N \approx 3 \times 10^{12}$ cm^{-3}, assuming that the effect of so low an impurity density ($< 10^{-3} n_s$, $10^{-4} n_0$) on the EHL parameters is negligible. However, since the EHL binding energy is small ($|\mu_L| - \Delta_M/2 \sim kT$), the presence of even so low an impurity density is significant in strongly compressed Ge⟨~100⟩ crystals. The difference between the emission spectra of Ge⟨~100⟩ crystals with $N = 3 \times 10^{11}$ cm^{-3} and 3×10^{12} cm^{-3} is observed at $P > 300$ MPa (Fig. 4). At $P \gtrsim 400$ MPa no clearly pronounced emission line of EHL is observed in the spectra of pure crystals up to the maximum excitation densities $W \approx 200$ W/cm^2, neither in the ordinary spectrum nor in the spectrum that is differential with respect to the excitation density [Fig. 4(b)]. At the same time the ratio I_{TA}/I_{LA} at $\hbar\omega < E_{ex}$ and $W \sim 200$ W/cm^2, just as for the L line in weakly doped crystals, is practically independent of $\hbar\omega$. When the excitation density is decreased, the narrowing of the emission line is accompanied by an increase of the ratio I_{TA}/I_{LA} on its red edge, and at $W \approx 70$ W/cm^2 it has the form typical of EM, which is shown in Fig. 2(c). From a comparison of the emission spectra of pure and of weakly doped crystals it is seen that in pure crystals one can obtain a noticeably larger I_M/I_{FE} ratio before the red tail of the M line begins to broaden strongly. If the broadening of the M line in pure crystals is also associated with the start of condensation into EHL, it follows from a comparison of I_M/I_{FE} that $|\mu_{ex}|$ in pure crystals at $T = 2$ K is smaller by at least 0.05 meV than in crystals with $N = 3 \times 10^{12}$ cm^{-3}. We note, however, that in this case the gas-phase density amounts already to $\sim 2.5 \times 10^{15}$ cm^{-3} ($r_s = 2.6$), and it is not excluded that the broadening of the M line is connected not with the start of the condensation into EHL, but with a sufficiently strong interaction in the exciton system at these densities.

We call attention to the qualitative difference between the behavior of the emission spectra of pure and weakly doped strongly compressed Ge⟨~100⟩ crystals in a magnetic field (Figs. 6 and 7). It is seen from Fig. 7 that the decrease of the intensity in the region of the L line in a magnetic field is noticeable in pure crystals, just as in Ge with $N = 3 \times 10^{12}$ cm^{-3}, at $P = 250$ MPa. However, at large deformations the radiation intensity in the region of the L line, on the contrary, increases with increasing magnetic field (curve 4 of Fig. 7). As noted above, in pure strongly compressed Ge⟨~100⟩ crystals, the emission of the gas phase predominates. Therefore to separate the line L we used 20% modulation of the exciting light [Fig. 4(b), curve 2]. The function $I_L(H)/I_L(0)$, however, remained the same as in the case of 100% modulation, in accord with the observed absence of a change in the emission line shape in fields $H \lesssim 0.6$ T (Fig. 6, curves 1a and 2a).

In light of the analysis of the influence of the magnetic field on the EHL stability in Ge⟨~100⟩, this behavior of the emission spectra is evidence that in pure Ge⟨~100⟩ crystals, at the investigated temperatures ($T \gtrsim 2$ K) and excitation densities ($W \lesssim 200$ W/cm^2), no metallic EHL is produced. On the other hand, two phenomena observed at high excitation densities, namely the broadening of the red edge of the M line and the constancy of the emission line shape in a weak magnetic field, cannot be explained within the framework of the model of a weakly interacting gas of excitons and EM. When the density of the gas of the excitons and EM increases to $r_s \approx 3$–2.5, when the average distance between the particles $\langle r \rangle \sim 1.6 r_s a_{ex}$ becomes comparable with the EM scattering length[6] a_s, the M line begins to broaden because of the smearing of the molecular states. It is not excluded that at such small r_s an important role is assumed by recombination of excitons with transfer of part of the energy to another exciton (or to a collective excitation). The dependence of the ratio I_{TA}/I_{LA} in the region $\hbar\omega < E_{ex}$ becomes less steep with further increase of the excitation density, thus indicating that smearing and dissociation of the bound excitonic state takes place at $r_s = 2.5$–2. Obviously, under these conditions one should not observe in a magnetic field a decrease in the radiation-intensity ratio $I(\hbar\omega < E_{ex})/I(\hbar\omega > E_{ex})$ typical of emission from a system of excitons and EM as well as of a system of excitons, EM, and a weakly bound EHL, as a result of the decrease of the stability of the EM and EHL in the magnetic field.

We note in conclusion that it is still impossible to draw final conclusions concerning the nature of the ground state of the e-h system from the results of our investigation of strongly compressed Ge⟨~100⟩ crystals at $T_{ex} \gtrsim 2$ K from the obtained upper limit of the chemical potential in the EHL at 2 K, $\mu_L(2\text{ K}) \gtrsim -0.28 \pm 0.05$ meV, with allowance for the temperature correction to μ_L (~0.1 meV) due to the entropy contribution to the free energy, it follows that at $T = 0$ K the binding energy of the excitons in EHL is $\varphi \lesssim 0.18$ meV $\approx 0.5\Delta_M$. To solve this problem it is necessary to lower the temperature to such a value that the gas of the excitons and EM remains weakly interacting until the chemical potential in the gas phase reaches the EM level ($\mu_{ex} = -\Delta_M/2$). Under these conditions, in the absence of condensation into the metallic phase, Bose-Einstein condensation of the EM should be observed. According to estimates, the temperatures needed for such measurements are $T_{ex} \lesssim 0.5$ K.

The authors are deeply grateful to V. G. Lysenko, E. A. Pashitskiĭ, and V. B. Timofeev for helpful discussions.

[1] In straight-band polar semiconductors, a very important role is played by polaron effects, which are not considered in the idealized model of Ref. 4.

[2] A deflection of approximately 3–5% away from the ⟨100⟩ axis is necessary to lift the degeneracy in the conduction band.

[3] If the variational wave function of Brinkman *et al.*[8] is used for the EM, a value 2.3 is obtained for α (V. M. Édel'shtein, cited in Ref. 16).

[4] The power of the incident 1.06 μm radiation amounted in this case to 3 W at an excitation spot ~1.5 mm^2. With further increase of the size of the excitation spot, the emis-

sion spectra did not change because of the large diffusion length of the $e-h$ pairs.

[5)] Since the deviation of the gas of excitons on EM at $r_s = 3.5 - 3$ was neglected in the calculation, so that p_g increased additionally with increasing density, the estimates obtained for the increases of n_g and μ_L can be only under-valued.

[6)] The value $a_s = 6.9a_{ex}$ obtained in Ref. 5 is over-estimated by approximately a factor of 2 because of an incorrect choice of the EM binding energy ($0.02R$ in place of $0.1R$).

[1]T. M. Rice, Sol. State Phys. **32**, 1 (1977).
[2]J. C. Hensel, T. G. Phillips, and G. A. Thomas, *ibid.* **32**, 87 (1977).
[3]V. S. Bagaev, T. I. Galkina, O. V. Gogolin, and L. V. Keldysh, Pis'ma Zh. Eksp. Teor. Fiz. **10**, 309 (1969) [JETP Lett. **10**, 195 (1969)].
[4]L. V. Keldysh and A. P. Silin, Zh. Eksp. Teor. Fiz. **69**, 1053 (1975) [Sov. Phys. JETP **42**, 535 (1975)].
[5]W. F. Brinkman and T. M. Rice, Phys. Rev. **B7**, 1508 (1973).
[6]P. Vashishta, P. Bhattacharyya, and K. S. Singwi, Phys. Rev. **B10**, 5108 (1973).
[7]P. Vashishta, S. G. Das, and K. S. Singwi, Phys. Rev. Lett. **34**, 911 (1974).
[8]W. F. Brinkman, T. M. Rice, and B. J. Bell, Phys. Rev. **B8**, 1570 (1972).
[9]V. D. Kulakovskiĭ, I. V. Kukushkin, and V. B. Timofeev, Zh. Eksp. Teor. Fiz. **81**, 684 (1981) [Sov. Phys. JETP **54**, 366 (1981)].
[10]B. J. Feldman, H.-h. Chou, and G. K. Wong, Sol. State Commun. **26**, 209 (1978).
[11]I. V. Kukushkin, V. D. Kulakovskiĭ, and V. B. Timofeev, Pis'ma Zh. Eksp. Teor. Fiz. **32**, 304 (1980) [JETP Lett. **32**, 280 (1980)].
[12]V. D. Kulakovskiĭ, A. V. Malyavkin, and V. B. Timofeev, Zh. Eksp. Teor. Fiz. **77**, 752 (1979) [Sov. Phys. JETP **50**, 380 (1979)].
[13]W. F. Brinkman and P. A. Lee, Phys. Rev. Lett. **31**, 237 (1973).
[14]M. Rössler and R. Zimmerman, Phys. Stat. Sol. (b). **67**, 525 (1975).
[15]K. S. Singwi, M. P. Tosi, R. H. Land, and A. Sjölander, Phys. Rev. **176**, 598 (1968).
[16]V. D. Kulakovskiĭ, I. V. Kukushkin, and V. B. Timofeev, Zh. Eksp. Teor. Fiz. **78**, 381 (1980) [Sov. Phys. JETP **51**, 191 (1980)].
[17]T. M. Rice, Nuovo Cimento **B23**, 226 (1974).
[18]E. A. Andryushin, V. S. Babichenko, L. V. Keldysh, T. A. Onishchenko, and A. P. Silin, Pis'ma Zh. Eksp. Teor. Fiz. **24**, 210 (1976) [JETP Lett. **24**, 185 (1976)].
[19]V. S. Bagaev, T. I. Galkina, and O. V. Gogolin, Proc. Tenth Int. Conf. on Phys. Semicond., Cambridge, Springfield, Va., 1970, p. 500.
[20]H. L. Störmer and R. V. Martin, Phys. Rev. **B20**, 4213 (1979).
[21]L. V. Keldysh and A. P. Silin, Fiz. Tverd. Tela (Leningrad) **15**, 1532 (1973) [Sov. Phys. Solid State **15**, 1026 (1973)].
[22]T. G. Tratas and V. M. Édel'shteĭn, Zh. Eksp. Teor. Fiz. **81**, 696 (1981) [Sov. Phys. JETP **54**, 372 (1981)].
[23]G. L. Bir and G. E. Pikus, Symmetry and Strain-Induced Effects in Semiconductors, Wiley, 1975.
[24]L. D. Landau and E. M. Lifshitz, Statistical Physics, Pergamon, 1980.

Translated by J. G. Adashko